Progress In Electromagnetics Research, Vol. 105, 93–102, 2010

DESIGN OF DUAL-BAND BANDPASS FILTERS USING A DUAL FEEDING STRUCTURE AND EMBEDDED UNIFORM IMPEDANCE RESONATORS

R.-Y. Yang

Department of Material Engineering
National Pingtung University of Science and Technology
No. 1, Syuefu Rd., Neipu, Pingtung 912, Taiwan

K. Hon

Department of Technology Electro-Optical Engineering
Southern Taiwan University
Taiwan

C.-Y. Hung

Department of Electronics Engineering and Computer Sciences
Tung-Fang Institute of Technology
No. 110, Tung-Fung Road, Hunei Shiang, Kaohsiung 829, Taiwan

C.-S. Ye

Department of Electrical Engineering
Institute of Microelectronics
National Cheng Kung University
No. 1, University Road, Tainan 701, Taiwan

Abstract—In this paper, a simple method and structure to design a dual-band bandpass filter (BPF) by using a dual feeding structure and embedded uniform impedance resonator (UIR) is presented. In this structure, two passbands can be designed individually and several transmission zeros can be created to improve the band selectivity and stopband performance. The first passband is determined by the dual feeding structure and the second passband is determined by the UIR. Moreover, by using the inter coupling in the UIR, the performance of the second passband can be easily tuned without degrading the first passband. In order to verify the design concept, two filter

Corresponding author: C.-Y. Hung (goliro.goliro@msa.hinet.net).

examples, including 0.9/1.575 GHz for multi-services communication and 2.4/5.7 GHz for wireless local area network (WLAN), are designed in this study. Experimental results of the fabricated samples show a good agreement with the simulated results.

1. INTRODUCTION

Microstrip dual-band bandpass filter (BPF) is a key component in a RF receiver for the growing wireless communication applications operating in multi-band, especially in the new developed wireless local area networks (WLANs) standards such as IEEE 802.11b/g (2.4 GHz) and IEEE 802.11a (5.2/5.7 GHz) specifications [1]. The challenges for to design a dual-band BPF are to achieve high passband selectivity, compact size and simple design procedure simultaneously.

In past, many design methods for dual-band BPF have been proposed [2–9]. The most well known method is using stepped impedance resonators (SIRs) to shift the spurious frequencies of the SIRs to create the second passband [2–9]. However, it is difficult to control the passbands individually by using the SIR, since the dual passbands response is synthesized by the two resonator responses synchronously. Recently, a dual band BPF with wide band and narrow band simultaneously was reported [10]. However, the design method is complex since the four SIRs are fabricated by using the multilayered technology. A miniature planar dual-band filter BPF using a dual feeding structure and embedded resonators was reported [11]. The advantage to use the dual feeding structure is that two transmission zeros can be created near the passband edges to have a wide stopband [11]. However, the embedded resonators are still the SIRs, which are required to tune the physical length and the impedance ratio to achieve the second passband, causing the complex design procedure.

In this article, we propose a simple method and structure to design a high performance dual-band bandpass filter (BPF) by using a dual feeding structure and embedded resonators. However, the embedded resonators are not the SIRs, while modified uniform impedance resonators (UIRs) having inter coupling structures are used to tune the second passband. It is shown that two passbands can be designed individually and several transmission zeros can be created to improve the band selectivity and stopband performance by using this proposed structure. The modified UIRs with parallel couple line section. The design procedure is addressed in detail and two filter examples, including 0.9/1.5 GHz for multi-service communication and

2.4/5.7 GHz for wireless local area network (WLAN), are designed. Especially, the high isolation between the first and second passband can be obtained.

2. DESIGN OF THE DUAL-BAND BANDPASS FILTER

Figure 1 shows the configuration of the dual band BPF using a dual feeding structure and UIRs having inter coupling structures. Two subsections in the proposed structure are shown in Fig. 2. The first passband is mainly determined by the dual feeding structure and the second passband can be created by using the embedded UIR and the frequency of the second passband is further tuned by tuning the inter coupling structures of the UIR. Since the two passbands can be designed individually, the design procedures are simple and listed below:

The first step is to design the first passband by designing the dual feeding structure with the suitable physical length;

The second step is to design the second passband by using the UIRs of half-wavelength embedded in the dual feeding structure to create the second passband; and

The final step is to tune the performance of the second band using the inter coupling lines in the UIRs.

In the first step, the dual feeding structure, as shown in Fig. 2(a), is employed in the fundamental filter structure, based on the theoretical

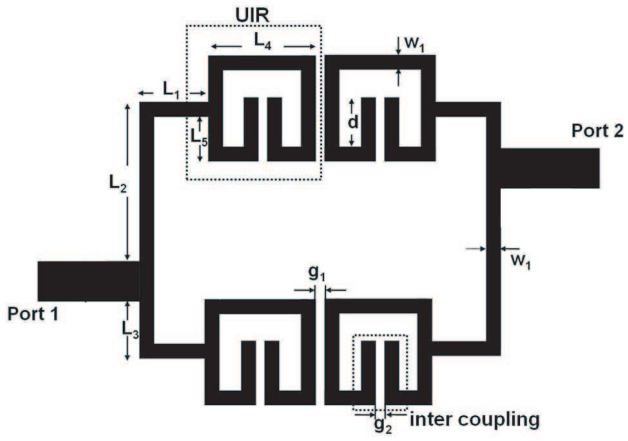

Figure 1. The configuration of the dual band BPF using a 0° feed structure and uniform impedance resonator (UIR).

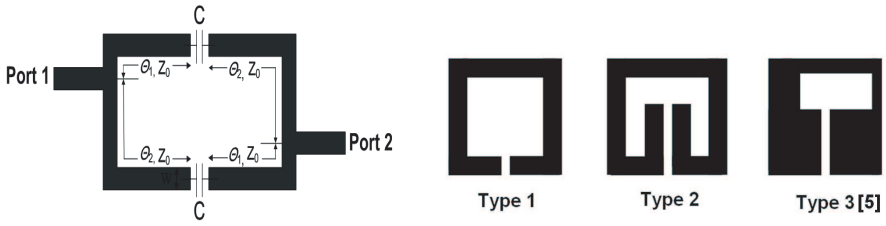

(a) (b)

Figure 2. The subsection in the proposed structure. (a) The primary structure of the resonator for the first passband and (b) three types of the embedded resonator for the second passband.

analysis reported in [11]. Two transmission lines with the characteristic impedance of 50 Ω are directly connected the resonators, acted as input and output (I/O) ports. It is reported the dual feeding structure can introduce the transmission zeros near the passband edge and the location of the transmission zero can be predicted by means of the typical transmission line theory of network conversion from the input admittance derivation. The transmission coefficient of the dual feeding structure is found as [11]:

$$S_{21} = \frac{j4\cos\theta_2}{\left(\frac{1}{Z_0\omega C}\cos\theta_2 - \sin\theta_2\right)^2 - 4} \tag{1}$$

where C is the capacitance between the terminals of the two resonators and Z_0 is the line impedance. The transmission zeros are created when θ_1 or θ_2 approaches $\pi/2$ to have the transmission coefficient $S_{21} = 0$. It is found the first two transmission zeros can be created if a 0° feed structure is used. These two zeros are close to and on the opposite sides of the first passband and, hence significantly increase the stopband rejection and passband selectivity [12]. The two transmission zeros at lower and higher frequency near the resonant frequency of the 0° feed structure are obtained when the length of θ_2 or θ_1 is a little bit shorter than the half-length of the 0° feed structure. With similar derivation, the locations of high order ones of the two transmission zeros can be also obtained near the second harmonic of the first passband frequency to construct a wide stopband because they are close to each other.

In the second step, the second passband is generated by using the UIRs of half-wavelength embedded in the dual feeding structure. It is noted that when the UIRs are embedded, the length of the dual feeding structure for generating the first passband must be reduced a length equal to the increment length (L_4) of the UIRs, as shown

in Fig. 1. Fig. 2(b) shows three types of the embedded resonator structures. Resonator of type 1 is the conventional open loop structure; resonator of type 2 is a type 1 having inter coupling structure and resonator of type 3 is the SIR structure used in [11]. It is known, however, resonator of type 3 is an asymmetry SIR and the design procedure is too complicated to flow since this structure is composed of multi-section transmission line of different impedance. For simplify the design procedure, resonators of the type 1 and type 2 are suitable for the design goal. The final step is to tune the performance of the second band using the inter coupling lines in the UIRs. Namely, The frequency adjustment is achieved by varying the length of the parallel coupled lines. For comparing the performance of the two type resonators, we design two filters to investigate the second passband response.

In this study, a full-wave EM simulator, IE3D [13] was employed for simulating and optimizing the filter design. The filter examples are realized using RT/Duroid 5880 substrate, which has a dielectric constant of $\varepsilon_r = 2.2$, a loss tangent of 0.0009 and a thickness h of 0.787 mm.

2.1. Filter Example I for WLAN

The filter example I is designed for WLAN, having the center frequencies of 2.4 and 5.7 GHz with 6% and 4% bandwidth, respectively. In the first step, simulated performance of the first passband of 2.4 GHz is shown in Fig. 3(a). The stopband is extended from 2.8 to 6.8 GHz with rejection greater than 25 dB. The good out-of-band rejection is very helpful for inserting the second passband within the stopband range to form a dual band behavior. In the second step, the simulated frequency responses of the proposed filter with resonators of type 1 and type 2 are shown in Fig. 3(b). It is clearly observed that the second passband can not be created when only using the type 1 resonator as the four embedded resonators since the coupling strength is not sufficient to excite the proper passband response. With the inter coupling introduced by the parallel couple line, the second passband response of 5.7 GHz with an extra transmission zero at the lower passband edge is obtained. Besides, the dimension of type 2 resonator is further miniaturized compared to the size of type 1 resonator, indicating that the type 2 resonators can not only provide dual band filter design but also achieve size reduction, compared with the resonators of type 1 and type 3. In the final step, the performance of the second band is tuned using the inter coupling lines in the UIRs. Fig. 3(c) shows simulated frequency response of the proposed filter with different lengths (d). It is observed that the central frequency of the second passband can be shifted from 5.7 GHz to 5.4 GHz as

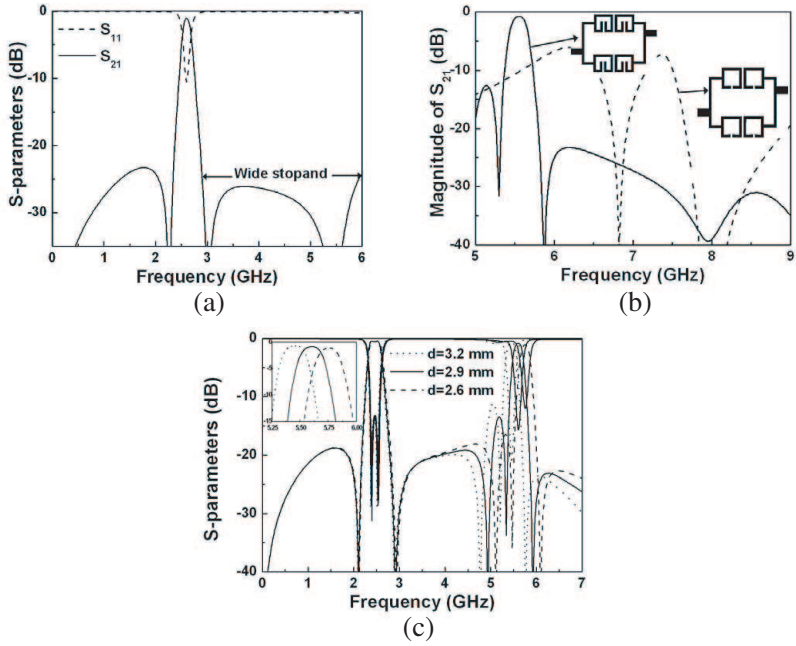

Figure 3. Filter example I for WLAN. Simulated performance of (a) the first passband and (b) second passband using type 1 and type 2, respectively, and (c) dual band response of the proposed filter with different coupling lengths d. The dimensions are $W_1 = 0.6$, $L_1 = 1.6$, $L_2 = 24.6$, $L_3 = 9.6$, $L_4 = 4.6$, $L_5 = 15$, $g_1 = 0.2$, $g_2 = 0.3$. All are in mm.

increasing the lengths d, but the first passband at 2.4 GHz is not affected. Moreover, the pair of transmission zeros near the second passband edges are moved synchronously. It is clearly verified that this high design freedom within the proposed circuit is achieved by means of varying the structure parameters to individually adjust the second passband frequency.

2.2. Filter Example II for GSM/GPS

In order to show the flexibility of the design procedure, the filter example II is designed for GSM/GPS, having the center frequencies of 0.9 and 1.575 GHz with 6% and 8% bandwidth, respectively. In this required targets, the good isolation between the two passbands is highly required since these two passabands are close. In the first step, the first passband of 0.9 GHz is generated by using the dual feeding

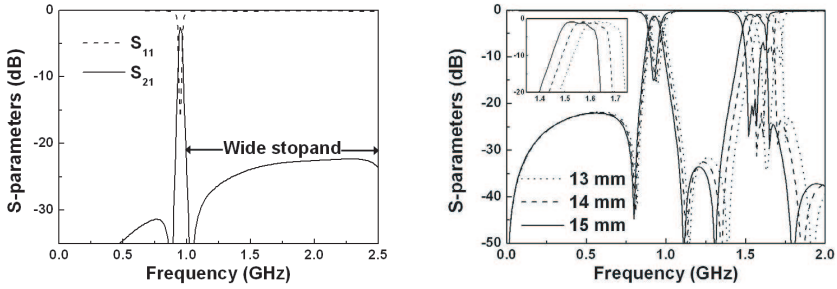

Figure 4. Filter example II for GSM/GPS. Simulated performance of (a) the first passband and (b) second pasband using type II with different coupling lengths d. The dimensions are $W_1 = 0.6$, $W_2 = 1.4$, $L_1 = 3.9$, $L_2 = 8.2$, $L_3 = 2$, $L_4 = 4.6$, $L_5 = 2$, $L_6 = 4$, $g_1 = 0.2$, $g_2 = 0.3$. All are in mm.

structure and simulated performance of the first passband is shown in Fig. 4(a). The stopband is extended from 1 to 2.5 GHz with rejection greater than 25 dB. After embedding the UIRs in the second step, the performance of the second band of 1.575 GHz is tuned using the inter coupling lines in the UIRs and the simulated frequency responses of the proposed filter with different lengths (d) is shown in Fig. 4(b). It is also again observed that the central frequency of the second passband can be tuned with different lengths d without affecting the first passband of 0.9 GHz. Fortunately, due to the multi-transmission zeros appeared near the passband edges to achieve a good band selectivity of the proposed design, a high isolation between two close passbands can be easily obtained, as shown in Fig. 4(b).

3. EXPERIMENTAL RESULTS AND DISCUSSION

The filter examples were fabricated and measured by an HP8510C Network Analyzer. Fig. 5(a) shows the photograph of the fabricated BPF sample I. The overall size is about 25 mm × 23 mm. The simulated and measured frequency responses are displayed in Fig. 5(b). The measured results have return loss of 21/10 dB, insertion loss of 0.5/2.2 dB, and FBW of 8/5% for 2.4/5.7 GHz, respectively. The transmission zeros are clearly observed at 2.13, 2.88, 5.25, 5.48 and 6.15 GHz, having attenuation levels of 43.9 dB, 41.5 dB, 41.5 dB, 36.8 dB and 46.2 dB, respectively. The transmission zeros actually provide an improved selectivity. The performances of the two

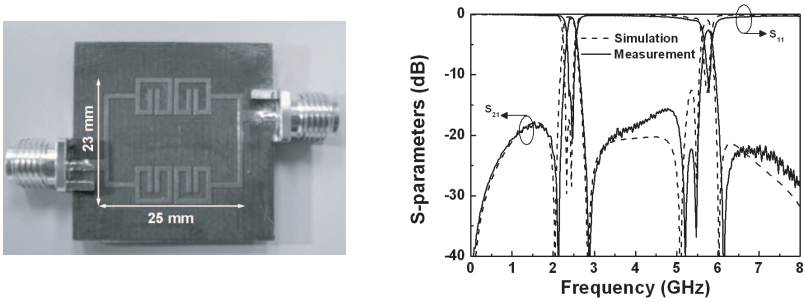

(a) (b)

Figure 5. (a) Photograph and (b) simulated and measured frequency responses of the fabricated dual-band BPF example I.

passbands are closely matched between the measured results and the simulated results, and some mismatch of frequency shift is due to the unpredictable fabrication error.

Figure 6(a) shows the photograph of the fabricated BPF sample II. The overall size is about 44 mm × 13 mm. The simulated and measured frequency responses are displayed in Fig. 6(b). The measured results have reture loss of 15/22 dB, insertion loss of 1.7/1.5 dB, and FBW of 6/7% for 0.9/1.575 GHz, respectively. The transmission zeros are clearly observed at 0.83, 1.12, 1.3, 1.8 and 2.23 GHz, having attenuation levels of 33.5 dB, 49.6 dB, 50.2 dB, 53.75 dB and 65.38 dB, respectively. With the help of the multi-transmission zeros appeared near the passband edges, a good band selectivity for two passbands and a high isolation between two close passbands can be easily obtained, as shown in Fig. 6(b). It is known the dual feeding structure can introduce the transmission zeros near the passband edge and the location of the transmission zero can be predicted by means of the Equation (1). Moreover, the inter coupling introduced by the parallel couple line can produce another extra transmission zeros near the passband edge, where the location of the transmission zeros depends on the coupling length of the embedded resonator. From these two examples, it is verified the proposed design concept provides a simple filter design and fabrication without using SIRs compared with the dual-band BPFs in the previous works [9, 10]. Moreover, the proposed design method for the dual-band BPF actually exhibits good performances including high band selectivity and in-band isolation.

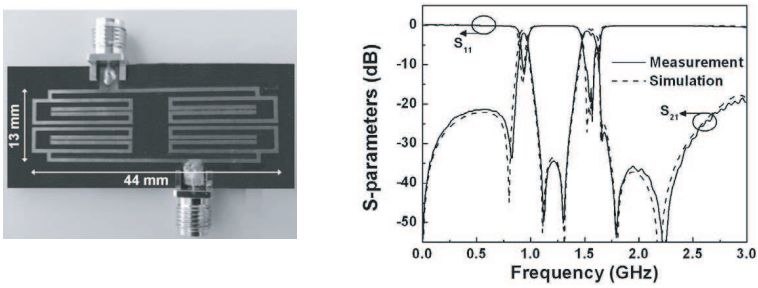

(a) (b)

Figure 6. (a) Photograph and (b) simulated and measured frequency responses of the fabricated dual-band BPF example II.

4. CONCLUSION

In this paper, we have presented a simple method and structure to design a dual-band BPF by using a dual feeding structure and embedded UIR. In this structure, two passbands can be designed individually and several transmission zeros can be created to improve the band selectivity and stopband performance. The first passband is determined by the dual feeding structure. Without increasing circuit size and complicated design procedures, the second passband can be tuned by adjusting the parallel coupled line length in the UIRs. Two filter examples, including 0.9/1.575 GHz for multi-services communication and 2.4/5.7 GHz for wireless local area network (WLAN), are designed In order to verify the design concept in this study. The measured results of two examples show a good agreement with the EM simulations. The proposed dual-band BPF is actually attractive for further development and applications in modern wireless communication systems.

REFERENCES

1. Hong, J. S. and M. J. Lancaster, *Microstrip Filters for RF/Microwave Applications*, John Wiley & Sons, Inc., New York, 2001.
2. Alkanhal, M. A. S., "Dual-band bandpass filters using inverted stepped-impedance resonators," *Journal of Electromagnetic Waves and Applications*, Vol. 23, Nos. 8–9, 1211–1220, 2009.
3. Lee, C. H., I. C. Wang, and C. I. G. Hsu, "Dual-band balanced BPF using $\lambda/4$ stepped-impedance resonators and folded

feed lines," *Journal of Electromagnetic Waves and Applications*, Vol. 23, Nos. 17–18, 2441–2449, 2009.

4. Wang, J. P., B.-Z. Wang, Y. X. Wang, and Y.-X. Guo, "Dual-band microstrip stepped-impedance bandpass filter with defected ground structure," *Journal of Electromagnetic Waves and Applications*, Vol. 22, No. 4, 463–470, 2008.
5. Weng, M. H., H. W. Wu, and Y. K. Su, "Compact and low loss dual-band bandpass filter using pseudo-interdigital stepped impedance resonators for WLANs," *IEEE Microw. Wireless Compon. Lett.*, Vol. 17, 187–189, 2007.
6. Chang, Y.-C., C.-H. Kao, M.-H. Weng, and R.-Y. Yang, "Design of the compact dual-band bandpass filter with high isolation for GPS/WLAN applications," *IEEE Microw. Wireless Compon. Lett.*, Vol. 19, 780–782, 2009.
7. Weng, M.-H., C.-H. Kao, and Y.-C. Chang, "A compact dual-band bandpass filter using cross-coupled asymmetric SIRs for WLANs," *Journal of Electromagnetic Waves and Applications*, Vol. 24, Nos. 2–3, 161–168, 2010.
8. Velazquez-Ahumada, M. D. C., J. Martel-Villagr, F. Medina, and F. Mesa, "Application of stub loaded folded stepped impedance resonators to dual band filter design," *Progress In Electromagnetic Research*, Vol. 102, 107–124, 2010.
9. Weng, M.-H., S.-K. Liu, H.-W. Wu, and C.-H. Hung, "A dual-band bandpass filter having wide and narrow bands simultaneously using multilayered stepped impedance resonators," *Progress In Electromagnetics Research Letters*, Vol. 13, 139–147, 2010.
10. Chen, C. Y., C. Y. Hsu, and H. R. Chuang, "Design of miniature planar dual-band filter using dual-feeding structures and embedded resonators," *IEEE Microw. Wireless Compon. Lett.*, Vol. 16, 669–671, 2006.
11. Tsai, C. M., S. Y. Lee, and C. C. Tsai, "Performance of a planar filter using a zero-degree feed structure," *IEEE Trans. Microw. Theory Tech.*, Vol. 50, 2362–2367, 2002.
12. Lee, S. Y. and C. M. Tsai, "New cross-coupled filter design using improved hairpin resonators," *IEEE Trans. Microw. Theory Tech.*, Vol. 48, 2482–2490, 2000.
13. IE3D Simulator, Zeland Software, Inc., 1997.